Jordan Journal of Civil Engineering, Volume **20**, No. **4**, **2026**
DOI: https://doi.org/10.14525/JJCE.v20i4.07

Jordan Journal of Civil Engineering

Journal homepage: https://jjce.just.edu.jo

Experimental Investigation of Velocity Distribution and Flow Resistance under Floating Vegetation

Adel A. Mahmoud [1)]

[1)] *Faculty of Engineering, Sohag University, Sohag 82524, Egypt. Email: adelahmed@eng.sohag.edu.eg*

ARTICLE INFO

Article History:
Received: 9/1/2026
Accepted: 16/6/2026

ABSTRACT

Floating aquatic vegetation, particularly water hyacinth (*Eichhornia crassipes*), significantly alters open channel hydraulics by introducing surface and subsurface flow resistance to the flow. This study experimentally investigates the influence of floating vegetation on the vertical distribution of streamwise velocity and flow resistance in an open channel flume using natural water hyacinth under varied conditions of vegetation densities and root depths. Vertical profiles of streamwise velocity were measured using a Pitot tube at multiple depths, and water surface elevations were recorded to evaluate flow resistance. The results reveal that floating vegetation alters vertical velocity profiles, forming an asymmetric velocity profile similar to that observed under ice covers or closed conduit flows. Vegetation density primarily controls surface blockage, while root depth governs vertical momentum redistribution, turbulence generation, and shear layer formation. Increasing vegetation density or root depth enhances flow resistance and intensifies turbulence near the upper flow region. These findings provide quantitative insights into the layered flow structure induced by floating vegetation, improving the understanding of energy dissipation, turbulence modulation, and resistance mechanisms. The results have practical implications for hydraulic modeling, vegetation management, and mitigation of flow obstruction in vegetated waterways.

Keywords: Floating vegetation, Water hyacinth, Vertical velocity distribution, Flow resistance, Turbulence, Open channel flow.

INTRODUCTION

Aquatic vegetation is common in both natural and constructed water systems,, such as rivers, lakes, wetlands, and, notably, irrigation canals (Chambers et al., 2008; Murphy et al., 2019). While it serves important ecological roles, such as providing habitat and affecting nutrient cycling (Carpenter and Lodge, 1986), its presence has a significant effect on channel hydraulics, producing considerable management issues (Green, 2005; Nepf, 2012).

Among the several types of aquatic vegetation, floating vegetation, which is defined by plants that grow primarily on the water surface and have root systems that extend below the water column (e.g., water hyacinth, duckweed, water lilies) (Wetzel, 2001), presents a unique set of hydraulic challenges (Urantinon & Pilailar, 2015; Mohamed et al., 2020; Wang et al., 2024 Li et al., 2025). Invasive and rapidly spreading species,, such as water hyacinth (*Eichhornia crassipes*), are particularly problematic globally, capable of forming dense mats that severely restrict flow, significantly reduce the conveyance capacity of water systems, increase flood risks by inducing significant backwater effects, and obstruct navigation and the proper functioning of hydraulic structures (Pieterse &

Murphy, 1990; Villamagna & Murphy, 2010; Li et al., 2020; Gui et al., 2024). Consequently, a detailed understanding and accurate quantification of the hydraulic impacts caused by floating vegetation are essential for the development of effective water resource management strategies, irrigation canal design, and efficient maintenance planning (Petryk & Bosmajian III, 1975).

Significant research efforts in recent decades have focused on clarifying the intricate relationships between different types of aquatic vegetation & open channel flow dynamics. Early studies demonstrated that vegetation enhances flow resistance, often expressed through increased Manning's roughness coefficients, Darcy-Weisbach friction factors or vegetation drag force (Chow, 1959; Yen, 2002, Xu et al., 2022; Ginting et al., 2025, Mahmoud & Uchida, 2026). Subsequent experimental and numerical studies have examined the impact of different vegetation characteristics, such as density, stem/root flexibility, spatial configuration, and submergence ratio, on essential flow parameters, including mean velocity distributions, turbulence structure, and drag forces (Wilson et al., 2003; Järvelä, 2004; Aberle & Järvelä, 2013; Vargas-Luna et al., 2015; Mahmoud & Uchida, 2024; Mahmoud et al., 2025; Mahmoud and Uchida, 2026). Studies focusing on flow cover vegetation, including Water Hyacinth or similar phenomena, such as ice covers, have repeatedly demonstrated significant changes to the vertical velocity profile. The introduction of shear resistance at the water surface moves the location of maximum velocity lower, away from the free surface, resulting in profiles that frequently resemble those seen in pipe flow (Huai et al., 2012; Urantinon & Pilailar, 2015; Han et al., 2018; Li et al., 2020; Gui et al., 2024). Urantinon and Pilailar (2015) and Mohamed et al. (2020) experimentally investigated the effects of water hyacinth on flow characteristics. They found that the presence of water hyacinth produces a significant heading up effect (an elevation in the water surface profile upstream of the vegetated area) and fundamentally alters the vertical velocity distribution.

Despite these advancements, many aspects of the hydraulic interactions between floating vegetation (water hyacinth) and open channel flow remain insufficiently explored, particularly regarding the combined influence of surface canopy coverage and subsurface root penetration on velocity distribution and turbulence structure. The dual resistance from floating mats and fibrous roots causes complex effects on flow due to the combined surface and subsurface resistance. While cumulative impacts of water hyacinth on bulk flow resistance are reasonably documented (Mohamed et al., 2020) and streamwise velocity characteristics are recognized (Urantinon & Pilailar, 2015), no study has simultaneously and systematically investigated how independently varying both vegetation density and root depth controls the layered velocity structure, flow resistance parameters, and turbulence behavior in open-channel flow using natural water hyacinth specimens. Moreover, earlier research used artificial vegetation or rigid elements to simplify plant morphology (Liu et al., 2010; Stone & Shen, 2002), neglecting the flexibility, buoyancy, and heterogeneous root structures of real floating vegetation, which play critical roles in flow-plant interaction and turbulence modulation (Vargas-Luna et al., 2015; Chen et al., 2018). The present study addresses this gap through a comprehensive series of controlled laboratory experiments.

The experiments were conducted using natural water hyacinth to investigate the hydrodynamic effects of floating vegetation under systematically varied conditions of vegetation density, root depth, and discharge. Vertical velocity profiles were measured using a Pitot tube at multiple depths, and water surface elevations were recorded to estimate flow resistance parameters. The study aims to examine how floating vegetation alters the overall flow structure, including vertical velocity distribution, resistance characteristics, and turbulence behavior in open-channel conditions. Through these analyses, the study seeks to enhance understanding of the interactions between surface and subsurface vegetation induced drag and their combined effects on flow dynamics, energy dissipation, and turbulence generation. The findings provide valuable insights for improving hydraulic modeling approaches, designing vegetation management strategies, and mitigating flow obstruction in vegetated waterways.

EXPERIMENTAL SETUP

The experimental investigation utilized a recirculating, horizontal, rectangular open-channel flume with dimensions of 10.0 m in length, 0.3 m in width, and 0.3 m in depth (Figure 1), and Manning roughness coefficient n=0.012 $m^{1/3}$/s. To ensure stable and controlled inflow, an upstream head tank supplied water to the flume. Flow depth adjustments were managed *via* a hinged, variable-sloping tailgate positioned at the flume's downstream exit.

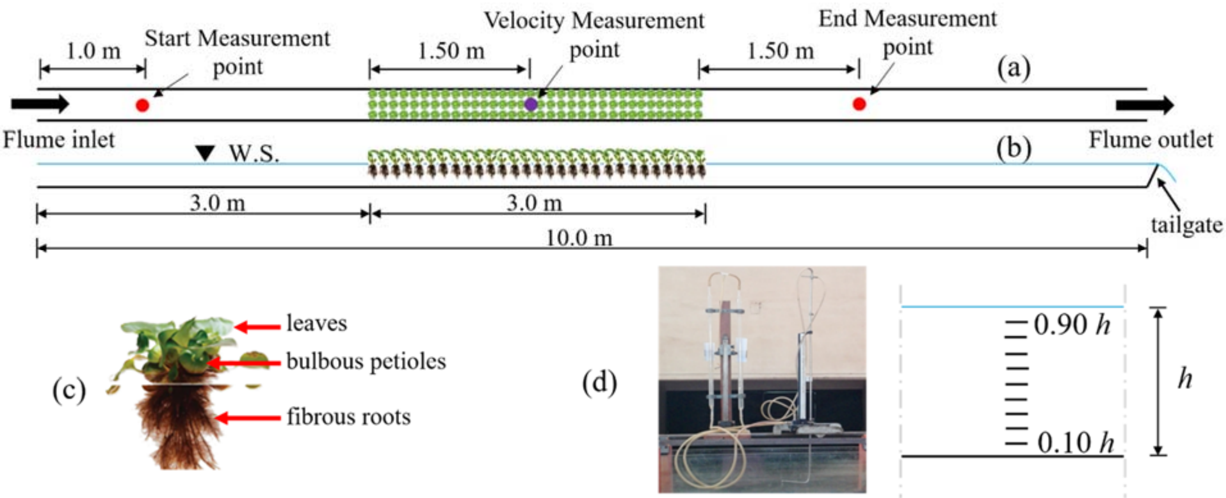

Figure 1. Experimental setup: (a) plan view of the flume showing the aligned vegetation arrangement, the longitudinal position of the velocity measurement section, and the start and end points of the water surface measurement range; (b) side view of the flume showing the position of water hyacinth plants relative to the water surface (W.S.); (c) main components of a water hyacinth plant; and (d) Pitot tube arrangement showing the vertical distribution of streamwise velocity measurement points within the flow depth *h*

Floating vegetation conditions were simulated using natural water hyacinth plants (*Eichhornia crassipes*), which were collected from local natural streams prior to the experiments. Structurally, water hyacinth exhibits bulbous petioles that ensure buoyancy at the water surface, horizontally and vertically spreading leaves, and dense fibrous roots extending into the flow (Gaurav et al., 2020) (Figure 1c), which enhance form resistance and turbulence generation in the subsurface region. The selected plants were positioned within the middle section of the flume, with a coverage length of 3.00 m, starting 3.0 m downstream from the channel entrance in aligned arrangement as shown in Figure 1a). To prevent the plants from drifting with the flow and maintain the desired densities, a support system was employed, as detailed by (Mohamed et al., 2020). This involved wooden frames (0.29 m wide, 1.00 m long) divided into smaller equal rectangles by fine cotton thread, within which the plants were placed. These frames were suspended approximately 2 cm above the water surface using fine cotton threads, minimizing retardation to the surface flow by the system itself. Preliminary tests conducted with the wooden frame alone (without any vegetation) showed that velocity profile deviations were less than 2%-3% compared to free-flow conditions, confirming that the frame itself introduces negligible additional hydraulic resistance.

Comprehensive experimental initial conditions were set up to investigate the influence of various vegetation and flow parameters, with the range of variables summarized in Table 1. Four different vegetation densities (λ) were tested: 30, 60, 90, and 120 plants/m². The effect of root penetration was examined using three distinct vegetation root depths (k_r): 1 cm, 3 cm, and 5 cm measured below water surface. The selected vegetation density range (30-120 plants/m²) and root depth range (1-5 cm) were chosen to represent the growth stages of water hyacinth from young to mature plants, consistent with field observations reported by Gaurav et al. (2020). For each configuration, a range of four flow discharges (Q) was passed through the flume: 10, 12, 14, and 16 L/s. All experimental conditions correspond to subcritical flow with Froude numbers in the range Fr = 0.14-0.22 and Reynolds numbers Re > 11,000, confirming fully turbulent flow. For each run series in Table 1, vegetation density was increased incrementally from 30 to 120 plants/m² by adding plants to the existing mat, while root depth and discharge were held constant. The root depth was then changed to the next level and the full density-discharge matrix was repeated. In addition to vegetated experimental runs, a baseline case without any water hyacinth was also performed under corresponding flow conditions for comparative analysis. These baseline free-flow experiments serve as the reference condition against which all vegetated cases are compared throughout the study, enabling direct quantification of the vegetation-induced increase in flow resistance parameters. The flow streamwise velocity is measured with a Pitot tube at the middle of the vegetation area (1.50 m downstream of vegetation beginning (Figure 1a) at different points in the vertical direction every 0.10 of water depth starting from channel bed to the water surface (Figure 1d). While water depths are measured with point gauges every 0.30 m along the flume outside and inside the vegetation area, the measurement sections extend from 1.0 m downstream of the channel inlet to 1.50 m beyond the vegetation area, as illustrated in Figure 1a. Measurement accuracy was assessed based on instrument specifications and repeatability of readings. For the point gauge, the accuracy is ±0.1 mm. For the Pitot tube, repeated readings at the same point under identical flow conditions yielded velocity values within ±2%-3% of the mean.

Table 1. Summary of experimental conditions

Run Series	Discharge Q (L/s)	Vegetation Density λ (plants/m²)	Root Depth k_r (cm)	Number of Runs
Baseline (no vegetation)	10, 12, 14, 16	—	—	4
Series 1	10, 12, 14, 16	30, 60, 90, 120	5 (fixed)	16
Series 2	10, 12, 14, 16	30, 60, 90, 120	3 (fixed)	16
Series 3	10, 12, 14, 16	30, 60, 90, 120	1 (fixed)	16
Total				52

RESULTS AND DISCUSSION

Vertical Distribution of Streamwise Velocity for Free-vegetation Cases

To first verify the accuracy of the experimental data, the vertical profiles of streamwise velocity obtained under free-flow conditions (without vegetation) for different discharges were compared with the theoretical logarithmic velocity distribution, as shown in Figure 2. The measurements were conducted at the same location used for vegetated cases; namely, 1.50 m downstream from the beginning of the vegetation section.

The logarithmic distribution of the streamwise velocity u, over a certain distance from the channel bottom z, commonly known as the general log law for turbulent boundary-layer flows, has been widely used to describe velocity profiles over smooth, transitional, and rough boundaries (Chow, 1959; Schlichting & Gersten, 2000; Nezu & Nakagawa, 1993).

$$u(z) = (u^*/\kappa)\, ln(z/z_0) \qquad (1)$$

where u^* is the bed friction velocity, $\kappa = 0.41$ is the von Kármán constant, and z_o is the roughness length. For the hydraulically smooth conditions of the present flume (smooth glass walls, $n = 0.012$ s/m$^{1/3}$), z_o is given by $z_o = 0.11\nu/u^*$, where ν is the kinematic viscosity of water.

As shown in Figure 2, the measured velocity profiles agree closely with the theoretical logarithmic distribution, yielding coefficients of determination (R^2) of 0.997, 0.997, 0.988, and 0.991 for discharges of Q=10,12,14, and 16 L/s, respectively. These results confirm the reliability and accuracy of the experimental data and the instruments employed in the present study.

Effect of Different Vegetation Densities and Root Depths on Vertical Profile of Streamwise Velocity

The presence of floating vegetation at the water surface forms a dense mat-like layer that alters the boundary conditions of open channel flow, effectively creating conditions similar to those of a nearly solid lid. Under such circumstances, the streamwise velocity close to the water surface equals zero, and the vertical velocity distribution deviates substantially from the classical logarithmic profile typical of free-surface flows (Figure 2). Instead, it tends to resemble the velocity structures observed in closed-conduit flows,, such as pipes, or in rivers under ice cover (Lau, 1982; Robert & Tran, 2012; Urantinon & Pilailar, 2015; Ai et al., 2020; Li et al., 2020). In these systems, the suppression of velocity at the top boundary shifts the location of maximum velocity downward into the water column, producing an asymmetric profile compared with closed-conduit flows.

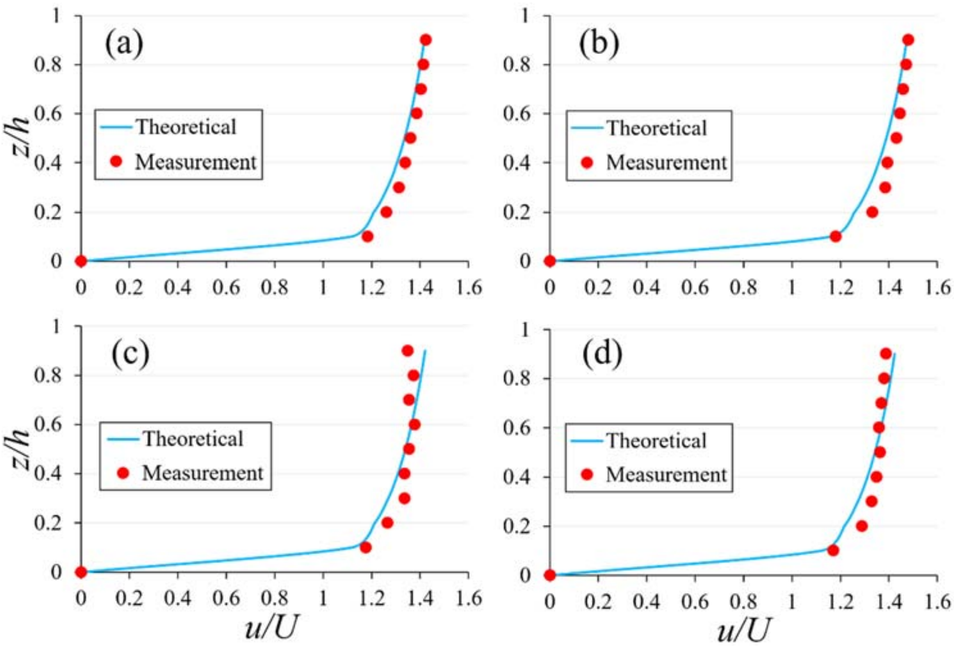

Figure 2. Vertical profiles of streamwise velocity for the free-flow cases at different inflow discharges: (a) 10 L/s, (b) 12 L/s, (c) 14 L/s, and (d) 16 L/s. *h* is water depth (m), and *U* is depth-averaged velocity (m/s)

For floating vegetation dominated by water hyacinth (*Eichhornia crassipes*) (Figure 1c), however, the hydraulic behavior is more complex. Unlike rigid lids or impermeable ice sheets, water hyacinths possess flexible stems and buoyant petioles that float on the surface while supporting trailing root systems beneath. The spacing between individual plants introduces partial porosity at the surface, allowing some flow to pass through the gaps, while the root systems penetrate into the water column to varying depths depending on plant maturity and environmental conditions. Consequently, the surface velocity between plants does not vanish entirely, but decreases substantially relative to the non-vegetated case, as confirmed in Figure 3. This intermediate condition, situated between an open free surface and a fully solid boundary, reflects the dual resistance exerted by the floating mat and the submerged roots (Urantinon & Pilailar, 2015; Nepf, 2012).

Systematic experiments were performed to isolate the effects of vegetation density and root depth. Figures 3a and 3b illustrate the influence of vegetation density at a constant root depth (k_r = 3 cm) under inflow discharges of 10 L/s and 16 L/s, respectively. Increasing the vegetation density reduces the spacing between plants, thereby decreasing the effective porosity of the floating mat. This leads to stronger blockage effects on the water surface, significantly reducing near-surface velocities. On the other hand, Figures 3c and 3d show the effect of increasing root depth while maintaining a constant vegetation density (λ = 90 plants/m²). Increasing the root depth introduces additional drag below the surface and enhances vertical momentum exchange, which also lowers the near-surface velocity, but to a larger degree.

A comparison between Figures 3a-b (density variation) and Figures 3c-d (root-depth variation) indicates that under the tested conditions, root depth exhibited a stronger influence on maximum velocity magnitude and location compared to vegetation density. This finding complements earlier studies, which showed that horizontal coverage primarily governs the overall flow resistance, whereas vertical penetration mainly modifies the turbulence structure and local shear layers (Tanino & Nepf, 2008; Huai et al., 2012; Vargas-Luna et al., 2015).

Overall, these results highlight the combined role of surface coverage and root penetration in shaping velocity distributions beneath floating vegetation mats. Vegetation density primarily governs the degree of surface blockage, thereby controlling how much flow can pass through the mat. In contrast, root depth influences how velocity gradients and shear are redistributed within the water column. Recognizing this distinction is essential for improving predictive models of vegetated flows and for assessing the hydraulic consequences of large-scale water hyacinth infestations in natural and engineered channels.

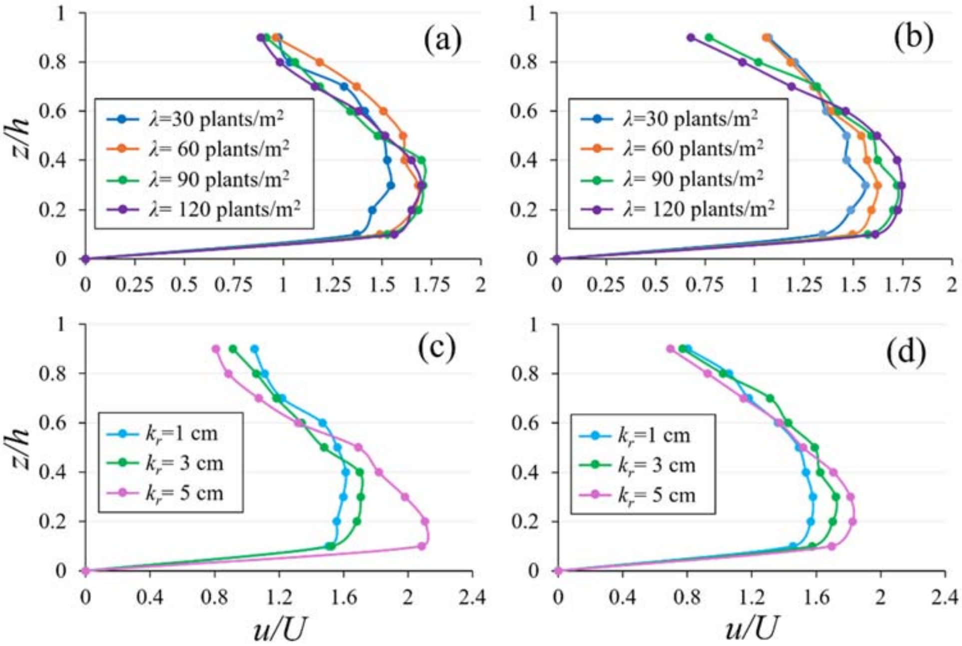

Figure 3. Vertical profiles of streamwise velocity under different inflow discharges: (a-b) effect of vegetation density at constant root depth (k_r = 3 cm) for 10 and 16 L/s, respectively; (c-d) effect of root depth at constant vegetation density (λ = 90 plants/m²) for 10 and 16 L/s, respectively.
Note: The horizontal axis ranges in panels (c) and (d) is wider than in panels (a) and (b) to accommodate the larger velocity magnification produced by deeper root penetration

Variation of Maximum Velocity with Vegetation Density and Root Depth

Figures 4 and 5 illustrate how the value and vertical position of the maximum streamwise velocity vary with vegetation density and root depth, respectively. In both cases, the introduction of floating vegetation induces a distinct downward shift of the maximum velocity from the free surface (Figure 2) toward the bed. The extent of this shift depends on both the density and vertical penetration of vegetation elements.

As shown in Figure 4(a), increasing vegetation density results in a gradual rise in the maximum velocity magnitude u_{max}. This trend can be attributed to the enhanced drag and blockage imposed by the densely packed water hyacinth mat on the surface. The floating canopy behaves like a rough, partially solid boundary that restricts flow passage near the surface and forces momentum to be concentrated within the lower water layers (Lau, 1982; Huai et al., 2012; Ai et al., 2020). The formation of a strong shear layer beneath the mat accelerates the mid-depth flow to compensate for the reduced conveyance at the surface. Correspondingly, Figure 4(b) shows that the location of the maximum velocity z_{max} moves downward with increasing density, reflecting the thickening of the surface shear layer and the increased resistance to near-surface motion (Tanino & Nepf, 2008; Nepf, 2012). In these tests, the root depth was constant at k_r =1 cm, ensuring that changes in velocity distribution primarily stem from surface-layer effects.

In comparison, vegetation root depth exerts a stronger influence on the velocity structure, as demonstrated in Figure 5. Increasing the penetration depth of roots introduces additional drag throughout the lower portion of the flow and modifies the vertical turbulence exchange. Figure 5(a) shows that deeper roots produce a more pronounced increase in maximum velocity magnitude. This is because the extended roots constrict the effective flow area, redirecting momentum into the unobstructed regions of the lower flow where velocity must increase to conserve discharge. Meanwhile, Figure 5(b) reveals a more substantial downward displacement of the maximum velocity with increasing root depth. This effect occurs, because root drag and turbulence damping expand the resistance zone vertically, forming an additional shear interface between the root tips and the lower clear-flow region (Stone & Shen, 2002; Liu et al., 2010). The roots also absorb part of the turbulent kinetic energy, reducing vertical mixing and allowing momentum to be redistributed in a more stratified manner (Vargas-Luna et al., 2015). For this set of experiments, vegetation density was kept constant at λ=60 plants/m^2.

To quantitatively support this observation, the percentage changes in maximum velocity magnitude and location were evaluated for both vegetation parameters. Increasing vegetation density from 30 to 120 plants/m² (at constant root depth k_r = 1 cm) produced an average increase in u_{max}/U of approximately 5%-16% across all discharge conditions, with a corresponding downward shift in z_{max}/h of only 0.1-0.2h. In contrast, increasing root depth from 1 cm to 5 cm (at constant vegetation density λ = 60 plants/m²) produced a more substantial increase in u_{max}/U of approximately 13%-40%, accompanied by a markedly larger downward shift in z_{max}/h of 0.2-0.4h. These results confirm that, under the tested conditions, root depth exerts a stronger influence on both the magnitude and location of the maximum velocity compared to vegetation density.

The relatively modest downward shift of maximum velocity location with increasing vegetation density (Figure 4b), compared with the more pronounced shift observed with root depth (Figure 5b), may partly reflect the limited density range examined (30 - 120 plants/m²). At higher densities, the floating mat approaches a quasi-solid impermeable boundary, which could potentially produce a more substantial displacement of the maximum velocity location, similar to the effect of increasing root depth. This hypothesis represents a promising direction for future investigation, particularly for natural water hyacinth infestations where densities may exceed those tested in the present study.

Taken together, Figures 4 and 5 highlight the layered nature of flow resistance under floating vegetation. The floating canopy generates a surface drag layer that induces shear and limits near-surface flow, while the submerged roots impose an additional resistance zone that dampens turbulence and shifts the maximum velocity downward. Although both parameters contribute to this behavior, root depth exerts the dominant control, because it directly modifies turbulence exchange and momentum distribution across the full flow depth. These results align with earlier studies showing that surface coverage primarily influences bulk flow resistance, whereas subsurface structures govern local velocity gradients and turbulence structure (Nepf, 2012; Okamoto & Nezu, 2013; Ai et al., 2020). Therefore, it is important to consider not only surface canopy cover, but also subsurface plant structures when assessing hydraulic resistance in floating vegetation conditions.

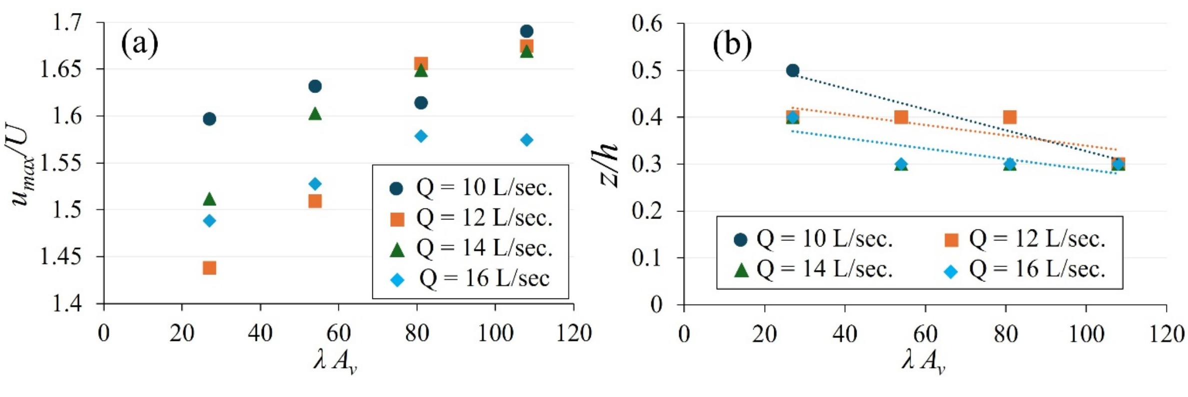

Figure 4. Effect of vegetation density on maximum velocity at a constant root depth (k_r=1 cm):
(a) value of maximum velocity u_{max},
(b) location of maximum velocity z_{max}. A_v is the vegetation coverage area

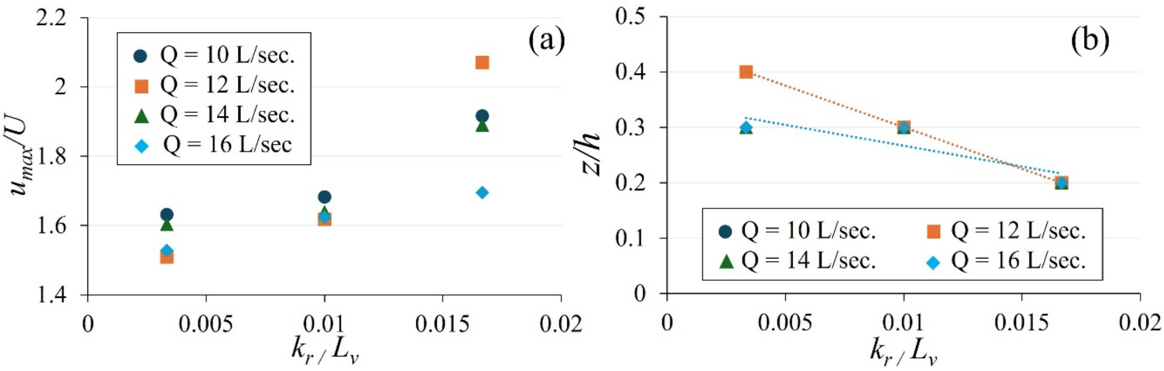

Figure 5. Effect of vegetation root depth on maximum velocity at a constant vegetation density (λ=60 plants/m^2): (a) value of maximum velocity, (b) location of maximum velocity. L_v =3.0 m is the vegetation coverage length

Flow Resistance Analysis

The flow resistance parameters were estimated based on the measured flow and water surface data for each experimental case. The bed shear stress (τ_b) was calculated using Eq. (2):

$$\tau_b = \rho g h S_f \tag{2}$$

where ρ is the fluid density, g is the gravitational acceleration, and S_f is the energy slope. The energy slope was evaluated from the measured energy loss (ΔH) across the vegetated section divided by its length (L_v), as:

$$S_f = \frac{\Delta H}{L_v}. \tag{3}$$

The Manning's roughness coefficient (n) was subsequently derived using the following relationships:

$$n = \frac{R_h^{2/3} S_f^{1/2}}{U} \tag{4}$$

where R_h is the hydraulic radius and U is the depth-averaged velocity.

The Manning's roughness coefficient n for the non-vegetated channel was determined experimentally for each baseline free-flow case (Table 1) using Eq. (4). The energy slope S_f was evaluated from water surface elevations measured by point gauges at two cross-sections separated by a known distance L, using Eq. (3). The resulting Manning's n values for the four baseline discharges ranged from 0.011 to 0.013 s/m$^{1/3}$, with a mean value of n = 0.012 s/m$^{1/3}$. This value is consistent with those reported in the literature for smooth glass-walled laboratory flumes (Chow, 1959; Nezu & Nakagawa, 1993), confirming the hydraulic smoothness of the channel bed and walls under non-vegetated conditions.

Figure 6 presents the variations of shear stress, and Manning's n values for different vegetation densities (λ) and root depths (k_r) under all discharge conditions considered in this study. Compared to the non-vegetated baseline values (n = 0.011-0.013 s/m$^{1/3}$, τ_b = 0.35-0.55 N/m²), the introduction of floating vegetation increases both parameters substantially across all tested conditions. The figure shows that increasing vegetation density or root depth results in a noticeable rise in the shear stress due to increasing the energy slope. This trend demonstrates that denser and deeper vegetation conditions impose greater hydraulic resistance on the flow. The elevated energy slope signifies higher head loss per unit channel length, while the corresponding increase in shear stress confirms that more momentum is dissipated through drag and turbulence within the vegetated section.

The increase in Manning's n with vegetation density and root depth further supports this observation. As vegetation becomes denser or root systems penetrate deeper, the flow passages between plants narrow, and the effective drag area increases. This enhances both form drag and frictional drag (due to increased turbulence and shear at the interfaces). The combined effect is a larger overall flow resistance, reflected in higher Manning's n values.

Physically, this means that floating vegetation reduces the hydraulic efficiency of the channel. A higher Manning's n corresponds to a lower flow conveyance capacity ($Q = 1/n \times A \times S_f^{1/2}$), meaning that the channel can carry less discharge for a given slope. As a result, backwater effects develop upstream of dense vegetation zones (Mohamed et al., 2020), potentially leading to localized flooding or waterlogging in irrigation networks. These effects become more pronounced as both vegetation density and root depth increase, consistent with the findings of previous studies (Petryk & Bosmajian, 1975; Green, 2005; Li et al., 2020).

Therefore, the observed rise in τ_b and n with vegetation parameters quantitatively confirms that floating vegetation significantly enhances flow resistance and energy dissipation in open channels. This highlights the importance of including vegetation-induced resistance in hydraulic design and maintenance strategies, particularly in regions affected by floating macrophytes, such as *Eichhornia crassipes*.

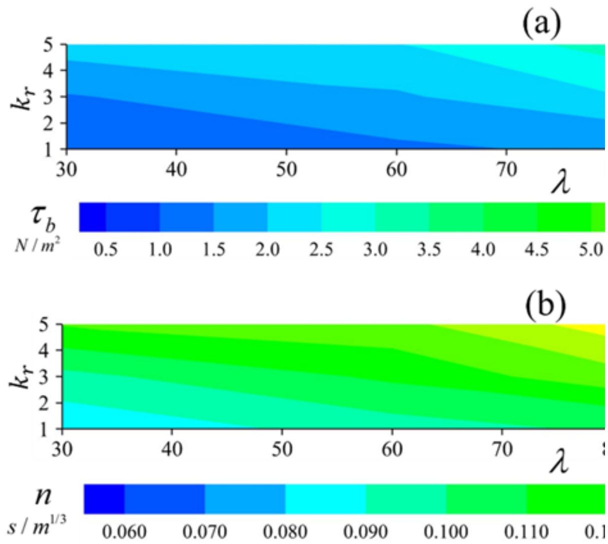

Figure 6. Variation of (a) bed shear stress (τ_b) and (b) Manning's roughness coefficient (n) with vegetation density and root depth for all discharge conditions considered in this study

Inferred Turbulence Characteristics from Velocity Gradients

Theoretical Background

Although direct turbulence measurements were not obtained in this study, the vertical profiles of streamwise velocity can be used to qualitatively infer the qualitative turbulence structure and momentum exchange mechanisms occurring within the floating vegetation region. The interaction between the floating mat of *Eichhornia crassipes* and the underlying flow creates a multi-layered shear system: a surface shear layer generated by the drag and partial blockage of the floating leaves and stems, and a root shear layer formed by the submerged fibrous roots that extend into the water column (Figure 7). Both layers strongly influence the vertical distribution of velocity gradients, turbulent kinetic energy (TKE), and Reynolds shear stress, ultimately modifying the energy dissipation and resistance characteristics of the channel (Nepf, 2012; Okamoto & Nezu, 2013; Li et al., 2020; Wang et al., 2022; Chen et al., 2026).

In open-channel flows, turbulence generation is primarily governed by the local velocity gradient, which controls the rate of shear deformation within the water column. The mean strain rate, *du/dz*, provides a direct indication of regions where turbulence is produced and energy is exchanged between mean flow and turbulent fluctuations.

According to the Boussinesq eddy-viscosity hypothesis, the turbulent Reynolds shear stress, τ_t, can be estimated as a function of the mean velocity gradient (Pope, 2000):

$$\tau_t = -\rho\overline{u'w'} = -\rho\nu_t\frac{du}{dz} \tag{5}$$

where $\overline{u'w'}$ denotes the covariance of velocity fluctuations in the streamwise and vertical directions, and ν_t is the eddy viscosity, representing the mixing efficiency of turbulent eddies.

The production of turbulent kinetic energy (TKE) per unit volume, P, quantifies the rate at which mean flow energy is converted into turbulence. It is given by the product of the Reynolds shear stress and the mean strain rate, representing the work done by turbulent stresses against the mean flow (Nezu & Nakagawa, 1993; Pope, 2000):

$$P = -\overline{u'w'}\frac{du}{dz}\,. \tag{6}$$

Substituting Eq. (5) into Eq. (6) yields the eddy-viscosity representation of the TKE production rate:

$$P = \rho\nu_t\left(\frac{du}{dz}\right)^2. \tag{7}$$

As indicated by Eq. (7), the TKE production rate is directly proportional to the square of the mean velocity gradient. Hence, even in the absence of direct turbulence measurements, the normalized term $(du/dz)^2$ can be used as a proxy for relative inferred turbulence production proxy P^*. This approach is commonly employed in studies of vegetated and complex environmental flows (Nezu & Nakagawa, 1993; Huai et al., 2012), providing qualitative insight into regions of enhanced mixing and momentum exchange.

Although $(du/dz)^2$ represents inferred turbulence production proxy only when variations in eddy viscosity ν_t are not dominant, ν_t in vegetated flows can vary due to shear intensity, vegetation drag, and mixing length scale, with spatial gradients inside and above the vegetation layer (Han et al., 2018). However, because the present study uses identical discharge range, flow depth, and channel geometry across all vegetation cases, the main variation in inferred turbulence production proxy is expected to arise from the vertical shear structure du/dz, which is influenced by vegetation density and root depth. Therefore, $(du/dz)^2$ is used here only as a qualitative indicator for comparing relative inferred turbulence production proxy among cases, and the conclusions are interpreted comparatively rather than quantitatively.

Following the approach of Han et al. (2018), the vertical flow domain in the present study, extending from the channel bed ($z = 0$) to the water surface ($z = h$), can be conceptually divided into two subregions based on the location of the maximum velocity (Z_{max}). As illustrated in Figure 7, these two subregions are: the bed zone, extending from the bed up to Z_{max}, and the vegetation zone, extending from Z_{max} to the water surface where the floating mat of *Eichhornia crassipes* is located.

The bed zone is primarily controlled by bottom roughness and bed shear stress, where turbulence is generated due to friction at the channel bed. In contrast, the vegetation zone is dominated by the resistance and drag imposed by the floating mat and submerged roots. The interface between these two regions occurs at the location of the maximum velocity, Z_{max}, marking the transition between bed generated and vegetation induced turbulence.

Because the velocity near the bed could not be directly measured due to instrument limitations (the minimum measurable distance from the bed $z_{min}= 0.2h =$ 1 - 2 cm), the present analysis focuses primarily on the vegetation zone, where turbulence generation is mainly controlled by vegetation induced shear rather than by bed friction. This focus helps isolate the effects of vegetation density and root depth on turbulence intensity and energy distribution without the confounding influence of near-bed turbulence.

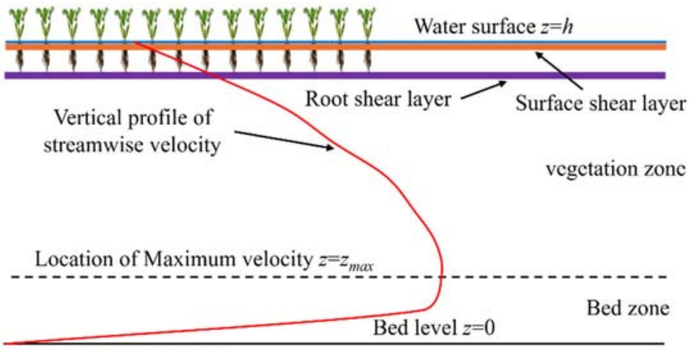

Figure 7. Schematic sketch showing the bed zone and vegetation zone, with surface and root shear layers formed beneath the water hyacinth

Comparison between Free-Flow and Floating Vegetation Cases

To further clarify the influence of floating vegetation on turbulence-related quantities, the velocity gradient du/dz and the inferred turbulence production proxy $P^* \propto (du/dz)^2$ for the floating-vegetation case (λ=90 plants/m^2, k_r=3 cm) were compared with their free-flow counterparts under the same discharge of 14 L/s (Figure 8). The comparison focuses exclusively on the vegetation zone (z / $h > Z_{max}/h$), where vegetation-induced drag dominates momentum exchange.

Despite having nearly identical depth-averaged velocities for both cases, the velocity profiles differ substantially in the upper portion of the flow. In the free-flow case, the velocity gradient du/dz gradually decreases toward the free surface, resulting in relatively low values of du/dz and thus weak inferred turbulence production proxy. In contrast, the floating-vegetation case exhibits a strong increase in $|du/dz|$ within the surface region, particularly between $z/h \approx 0.70$ and the vegetation canopy, where the measured velocity decreases sharply due to the drag imposed by the floating leaves and stems. This enhanced shear directly translates into higher inferred turbulence production proxy, as shown in Figure 8(b), reflecting more intense momentum extraction from the mean flow.

These patterns support the physical picture described earlier: the floating vegetation introduces a surface shear layer that is absent in free flow. Even though the roots in this case extend only 3 cm below the surface, they are sufficient to create a localized high-shear region that elevates inferred turbulence production proxy near the canopy. As a result, turbulence is shifted upward in the water column, rather than being concentrated near the bed as in the free-flow condition. This redistribution of turbulence helps explain the increased flow resistance and reduced conveyance observed under floating-vegetation conditions.

From Figure 8, it is evident that floating vegetation fundamentally alters the qualitative turbulence structure by enhancing shear and inferred turbulence production proxy in the upper flow region, whereas the free-flow case remains dominated by near-bed turbulence and retains a much smoother surface velocity profile.

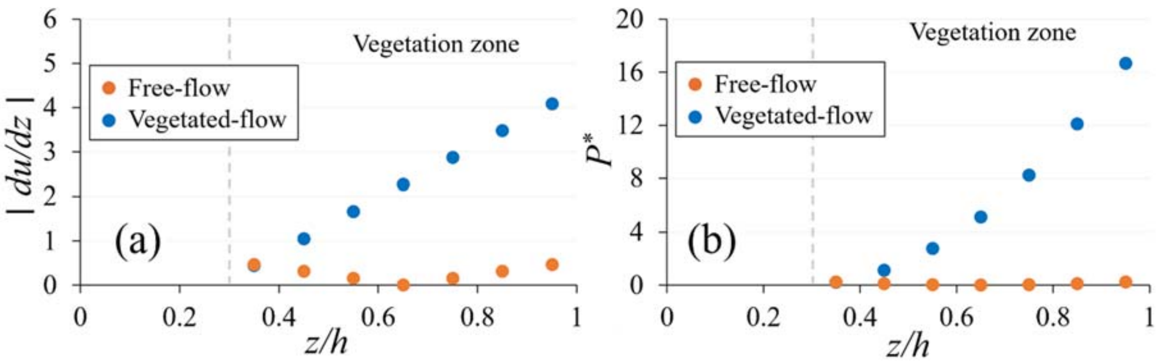

Figure 8. Comparison of (a) velocity gradient $|du/dz|$ and (b) inferred turbulence production $P^* \propto (du/dz)^2$ within the vegetation zone between free-flow and floating-vegetation cases (λ=90 plants/m², k_r=3 cm) under discharge =14 L/s

Effect of Vegetation Density and Root Depth on Turbulence

Figures 9 and 10 illustrate the influence of vegetation density and root depth on the velocity gradient du/dz and the inferred turbulence-production proxy $P^* \propto (du/dz)^2$ within the vegetation zone under a discharge of 16 L/s. To minimize experimental noise, the velocity profiles were first smoothed, allowing the underlying hydrodynamic trends to be identified with confidence.

Figure 9 presents the influence of vegetation density on the velocity gradient and inferred turbulence production proxy under constant root depth of 3 cm. After smoothing the velocity profiles, a clear and consistent pattern emerges where both du/dz and the inferred production term $P^* \propto (du/dz)^2$ increase systematically with density. Higher vegetation densities produce stronger surface-shear layers, as the floating leaves and stems impose greater drag and induce a sharper velocity deficit immediately beneath the mat. As density increases from 30 to 120 plants/m², the magnitude of P^* becomes progressively larger and more concentrated near the canopy, reflecting intensified momentum extraction and enhanced turbulence generation by the vegetation. These trends are consistent with the expected physical behavior, where increased frontal area, blockage, and stiffness of denser floating mats enhance vertical shear. The upward shift in inferred turbulence production proxy with increasing density therefore arises from stronger vegetation-induced resistance rather than measurement variability, confirming the dominant role of canopy density in controlling near-surface turbulence.

Figure 10 illustrates the influence of root depth on the velocity gradient and turbulence-production proxy for a constant density of 120 plants/m². The results show that deeper roots substantially intensify shear within the vegetation zone and alter its vertical structure. As root depth increases, the vegetation zone itself extends farther downward, enlarging the portion of the water column directly affected by vegetation drag. This expansion leads to a larger and more sustained velocity deficit beneath the floating mat, producing stronger vertical shear across a deeper region. Consequently, both the velocity gradient and the turbulence-production proxy P^*increase not only in magnitude, but also in vertical extent. For the deepest root condition (5 cm), elevated P^* values persist well below the canopy, reflecting the longer drag-producing layer introduced by the extended root system. This enhanced turbulence generation arises, because deeper roots increase frontal area exposure, intensify momentum extraction, and interact with a greater portion of the mean flow. As a result, root penetration depth emerges as a key control on the magnitude and distribution of turbulence beneath floating vegetation, with deeper roots producing stronger and more vertically distributed shear.

The present findings have direct practical implications for the design and management of vegetated waterways. The observed increase in Manning's n from 0.012 (non-vegetated) to values exceeding 0.15 under dense, deep-rooted conditions indicates a reduction in channel conveyance capacity, which has critical implications for irrigation canal design and flood risk assessment. Water resource managers should consider vegetation density and root depth thresholds when planning removal or control interventions for water hyacinth infestations. Furthermore, the measured velocity profiles and resistance parameters provide useful benchmark data for calibrating and validating numerical models of floating vegetation hydraulics.

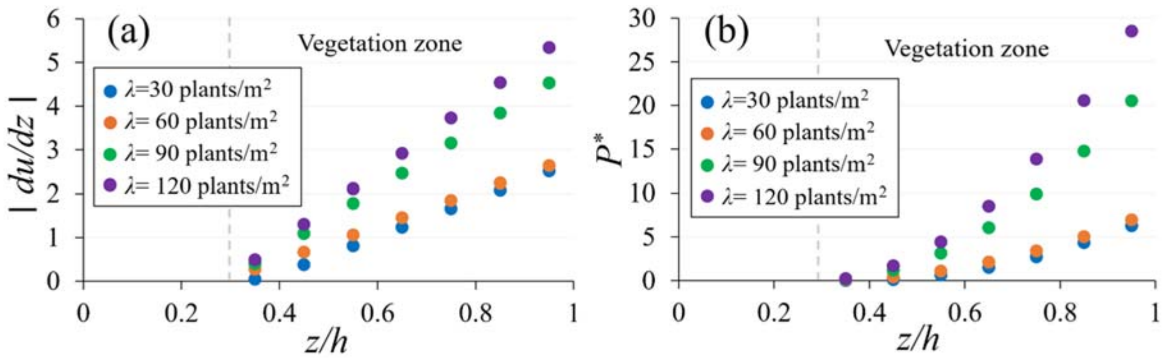

Figure 9. Effect of vegetation density on (a) velocity gradient du/dz and (b) inferred turbulence production $P^* \propto (du/dz)^2$ within the vegetation zone under *Q*=16 L/s for k_r=3cm

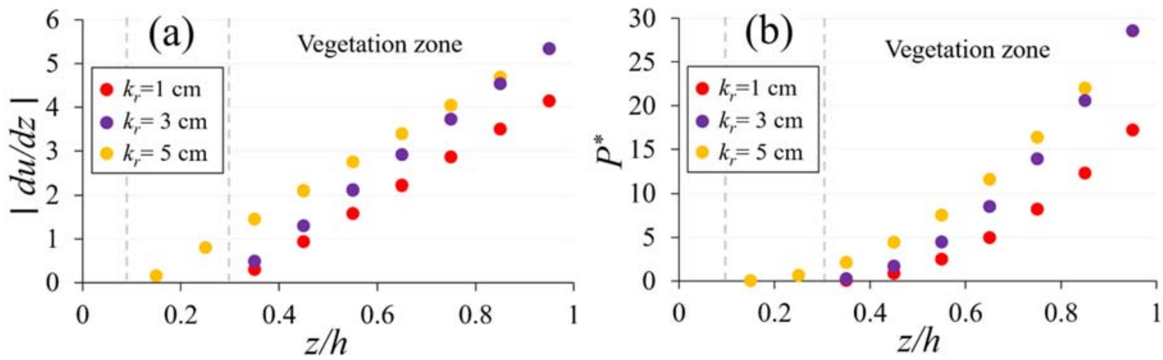

Figure 10. Effect of root depth on (a) velocity gradient $\mathrm{du/dz}$ and (b) inferred turbulence production $P^* \propto (du/dz)^2$ within the vegetation zone under *Q*=16L/s for *λ*=120 plants/m²

CONCLUSION

This study experimentally examined how floating water hyacinth influences open-channel flow structure, inferred turbulence characteristics, and hydraulic resistance. The results show that floating vegetation produces a distinctly layered velocity profile, with a downward shift of the maximum velocity caused by the combined drag of the surface canopy and submerged roots. Vegetation density primarily increases surface blockage, while root depth plays a stronger role by deepening the resistance zone, intensifying vertical shear, and enhancing the inferred turbulence production proxy near the upper flow region.

Both vegetation parameters lead to higher shear stress, energy slope, and Manning's n, confirming that floating vegetation significantly increases flow resistance and reduces channel conveyance capacity. These effects become more pronounced as vegetation mats thicken or roots extend farther into the water column. Overall, the findings highlight the importance of considering both canopy coverage and root penetration when predicting flow behavior in vegetated waterways and provide useful insights for hydraulic modeling, waterway management, and mitigation of floating vegetation impacts.

While the present study offers valuable qualitative understanding of turbulence redistribution through velocity-gradient analysis, definitive quantification of turbulence intensities and Reynolds stresses requires future investigation with direct turbulence measurement instrumentation. Finally, it should be noted that all experiments were conducted using an aligned vegetation arrangement, which was deliberately chosen to provide a controlled configuration for isolating the effects of density and root depth. In natural waterways, water hyacinth typically forms irregular, non-aligned patches that may produce different magnitudes of flow resistance and inferred turbulence production proxy production due to altered wake interaction patterns. Future studies should therefore investigate staggered and random vegetation arrangements to broaden the generalizability of the present findings to natural vegetated waterways.

REFERENCES

Aberle, J., & Järvelä, J. (2013). Flow resistance of emergent rigid and flexible floodplain vegetation. *Journal of Hydraulic Research*, *51*(1), 33-45. https://doi.org/10.1080/00221686.2012.754795

Ai, Y., Liu, M., & Huai, W. (2020). Numerical investigation of flow with floating vegetation island. *Journal of Hydrodynamics*, *32*(1), 31-43. https://doi.org/10.1007/s42241-020-0004-6

Carpenter, S.R., & Lodge, D.M. (1986). Effects of submersed macrophytes on ecosystem processes. *Aquatic Botany*, *26*, 341-370. https://doi.org/10.1016/0304-3770(86)90031-8

Chambers, P.A., Lacoul, P., Murphy, K.J., & Thomaz, S.M. (2008). Global diversity of aquatic macrophytes in freshwater. *Hydrobiologia*, *595*(1), 9-26. https://doi.org/10.1007/s10750-007-9154-6

Chen, X., Xu, D., Ji, C., & Zhang, Z. (2026). Shear-layer turbulence and drag in submerged flexible canopies with lateral sway. *Physics of Fluids*, *38*(4), 045127. https://doi.org/10.1063/5.0321487

Chow, V.T. (1959). *Open channel hydraulics.* McGraw-Hill International.

Gaurav, G.K., Mehmood, T., Cheng, L., Klemeš, J.J., & Shrivastava, D.K. (2020). Water hyacinth as a biomass: A review. *Journal of Cleaner Production*, *277*, 122214. https://doi.org/10.1016/j.jclepro.2020.122214

Ginting, B.M., Mahmoud, A.A., & Uchida, T. (2025). Semi-implicit model for bed friction and drag force terms with bottom pressure calculation in simulating dam-break flows with vegetation. *Journal of JSCE*, *13*(2), 24-16142. https://doi.org/10.2208/journalofjsce.24-16142

Green, J. C. (2005). Modeling flow resistance in vegetated streams: Review and development of new theory. *Hydrological Processes*, *19*(6), 1245-1259. https://doi.org/10.1002/hyp.5564

Gui, Z., Shan, Y., & Liu, C. (2024). Flow velocity adjustment in a channel with a floating vegetation canopy. *Journal of Hydrology*, *628*, 130528. https://doi.org/10.1016/j.jhydrol.2023.130528

Han, L., Zeng, Y., Chen, L., & Li, M. (2018). Modeling streamwise velocity and boundary shear stress of vegetation-covered flow. *Ecological Indicators*, *92*, 379-387. https://doi.org/10.1016/j.ecolind.2017.04.012

Huai, W., Hu, Y., Zeng, Y., & Han, J. (2012). Velocity distribution for open channel flows with suspended vegetation. *Advances in Water Resources*, *49*, 56-61. https://doi.org/10.1016/j.advwatres.2012.07.001

Järvelä, J. (2004). Determination of flow resistance caused by non-submerged woody vegetation. *International Journal of River Basin Management*, *2*(1), 61-70. https://doi.org/10.1080/15715124.2004.9635222

Lau, Y.L. (1982). Velocity distributions under floating covers. *Canadian Journal of Civil Engineering*, *9*(1), 76-83. https://doi.org/doi.org/10.1139/l82-008

Li, C., Gui, Z., Sun, S., Shan, Y., Wu, B., & Liu, C. (2025). Sediment deposition in a channel with floating vegetation based on a random displacement model. *Journal of Hydrodynamics*, *37*(3), 569-583. https://doi.org/10.1007/s42241-025-0038-x

Li, Q., Zeng, Y., & Zha, W. (2020). Velocity distribution and turbulence structure of open channel flow with floating-leaved vegetation. *Journal of Hydrology*, *590*, 125298. https://doi.org/10.1016/j.jhydrol.2020.125298

Liu, D., Diplas, P., Hodges, C.C., & Fairbanks, J.D. (2010). Hydrodynamics of flow through double layer rigid vegetation. *Geomorphology*, *116*(3-4), 286-296. https://doi.org/10.1016/j.geomorph.2009.11.024

Mahmoud, A.A., Ginting, B.M., & Uchida, T. (2025). Experimental investigation and numerical modeling of dam break flows over movable bed with vegetation. *Journal of JSCE*, *13*(1). https://doi.org/doi.org/10.2208/journalofjsce.24-00154

Mahmoud, A.A., & Uchida, T. (2024). Dam break flow through rigid-emergent vegetation. *Experiments in Fluids*, *65*(11), 1-14. https://doi.org/doi.org/10.1007/s00348-024-03901-1

Mahmoud, A.A., & Uchida, T. (2026). An unsteady drag force model for simulating dam break flows through rigid emergent vegetation. *Journal of Hydrology*, *664* (Part A), 134414. https://doi.org/10.1016/j.jhydrol.2025.134414

Mohamed, H.I., Abd-Elaal, A.-E.M., & Mahmoud, A.A. (2020). Flow characteristics of open channels with floating vegetation. *JES. Journal of Engineering Sciences*, *48*(2), 186-196. https://doi.org/10.21608/jesaun..2020.108332

Murphy, K., Efremov, A., Davidson, T.A., Molina-Navarro, E., Fidanza, K., Crivelari Betiol, T.C., Chambers, P., Tapia Grimaldo, J., Varandas Martins, S., Springuel, I., Kennedy, M., Mormul, R. P., Dibble, E., Hofstra, D., Lukács, B.A., Gebler, D., Baastrup-Spohr, L., & Urrutia-Estrada, J. (2019). World distribution, diversity and endemism of aquatic macrophytes. *Aquatic Botany*, *158*, 103127. https://doi.org/10.1016/j.aquabot.2019.06.006

Nepf, H.M. (2012). Hydrodynamics of vegetated channels. *Journal of Hydraulic Research*, *50*(3), 262-279. https://doi.org/10.1080/00221686.2012.696559

Nezu, I., & Nakagawa, H. (1993). *Turbulence in open channel flows*. A.A Balkema.

Okamoto, T., & Nezu, I. (2013). Spatial evolution of coherent motions in finite-length vegetation patch flow. *Environmental Fluid Mechanics*, *13*, 417-434. https://doi.org/doi.org/10.1007/s10652-013-9275-6

Petryk, S., & Bosmajian III, G. (1975). Analysis of flow through vegetation. *Journal of the Hydraulics Division*, *101*(7), 871-884. https://doi.org/doi:10.1061/JYCEAJ.0004397

Pieterse, A.H., & Murphy, K.J. (1990). *Aquatic weeds: The ecology and management of nuisance aquatic vegetation*. Oxford University Press.

Pope, S.B. (2000). *Turbulent flows*. Cambridge University Press.

Robert, A., & Tran, T. (2012). Mean and turbulent flow fields in a simulated ice-covered channel with a gravel bed: Some laboratory observations. *Earth Surface Processes and Landforms*, *37*(9), 951-956. https://doi.org/10.1002/esp.3211

Schlichting, H., & Gersten, K. (2000). *Boundary layer theory* (8th ed.). Springer-Verlag.

Stone, B.M., & Shen, H.T. (2002). Hydraulic resistance of flow in channels with cylindrical roughness. *Journal of Hydraulic Engineering*, *128*(5), 500-506. https://doi.org/10.1061/(ASCE)0733-9429(2002) 128:5(500)

Tanino, Y., & Nepf, H.M. (2008). Laboratory investigation of mean drag in a random array of rigid, emergent cylinders. *Journal of Hydraulic Engineering*, *134*(1), 34-41. https://doi.org/10.1061/(ASCE)0733-9429(2008)134:1(34)

Urantinon, A., & Pilailar, S. (2015). Effect of Water Hyacinth on Open-Channel Water Flow Behavior: Laboratory Scale. *Agriculture and Natural Resources*, *49*(6), 913-923. https://li01.tci-thaijo.org/index.php/anres/article/view/243794

Vargas-Luna, A., Crosato, A., & Uijttewaal, W.S.J. (2015). Effects of vegetation on flow and sediment transport: Comparative analyses and validation of predicting models. *Earth Surface Processes and Landforms*, *40*(2), 157-176. https://doi.org/10.1002/esp.3633

Villamagna, A.M., & Murphy, B.R. (2010). Ecological and socio-economic impacts of invasive water hyacinth (*Eichhornia crassipes*): A review. *Freshwater Biology*, *55*(2), 282-298. https://doi.org/10.1111/j.1365-2427.2009.02294.x

Wang, J., He, G., Dey, S., & Fang, H. (2022). Influence of submerged flexible vegetation on turbulence in an open-channel flow. *Journal of Fluid Mechanics*, *947*, A31. https://doi.org/10.1017/jfm.2022.598

Wetzel, R.G. (2001). *Limnology: Lake and river ecosystems* (3rd ed). Academic Press.

Wilson, C.A.M.E., Stoesser, T., Bates, P.D., & Pinzen, A.B. (2003). Open Channel flow through different forms of submerged flexible vegetation. *Journal of Hydraulic Engineering*, *129*(11), 847-853. https://doi.org/10.1061/(ASCE)0733-9429(2003)129: 11(847)

Xu, D., Liu, J., Wu, Y., & Ji, C. (2022). Numerical investigation of the dynamics of flexible vegetations in turbulent open-channel flows. *Journal of Hydrodynamics*, *34*(4), 681-699. https://doi.org/10.1007/s42241-022-0057-9

Yen, B.C. (2002). Open channel flow resistance. *Journal of Hydraulic Engineering*, *128*(1), 20-39. https://doi.org/doi:10.1061/(ASCE)0733-9429(2002) 128:1(20)